Interaction of Diethyldithiocarbamate with *n*-Type Cadmium Sulfide and Cadmium Selenide: Efficient Photoelectrochemical Oxidation to the Disulfide and Flat-Band Potential of the Semiconductor as a Function of Adsorbate Concentration

James W. Thackeray, Michael J. Natan, Pohleng Ng, and Mark S. Wrighton*

Contribution from the Department of Chemistry, Massachusetts Institute of Technology, Cambridge, Massachusetts 02139. *Received December 9, 1985*

Abstract: The behavior of sodium diethyldithiocarbamate, $Na[Et_2NCS_2]$, at n-type semiconducting CdX (X = S, Se) in CH_3CN/0.2 M $NaClO_4$ has been studied. The $Et_2NCS_2^-$ interacts strongly with the CdX surface and shifts the flat-band potential, E_{FB}, up to 1.0 V more negative with increasing $Et_2NCS_2^-$ concentration. The concentration dependence of the shift in E_{FB} has been studied in the range 0–0.2 M, with 0.01 M $Et_2NCS_2^-$ being sufficient to shift E_{FB} the maximum amount. The shift in E_{FB} is due to excess negative charge on the CdX surface due to the presence of adsorbed dithiocarbamate. The shift in E_{FB} is assumed to be proportional to $Et_2NCS_2^-$ coverage. A plot of change of E_{FB} with change in bulk concentration of $Et_2NCS_2^-$ can be modeled by using Langmuir adsorption isotherms. Adsorption data for two bis(dithiocarbamates), $Na^+_2[CH_2N(Et)CS_2^-]_2$ and $Na^+_2[CH_2CH_2CH_2N(Me)CS_2^-]_2$, show that maximum shifts of E_{FB} are obtained at lower solution concentrations than for $Et_2NCS_2^-$. The data show that the equilibrium constant for dithiocarbamate binding is somewhat greater (by a factor of 2) for CdS than CdSe. The value of E_{FB} in the presence of 0.2 M $Et_2NCS_2^-$ measured by interfacial capacitance accords well with the electrode potential corresponding to onset of photoelectrochemical oxidation upon illumination with light of energy greater than the band gap, E_g, of the semiconductor. High current efficiency (at least 98%) can be maintained to large extent conversion (70%) in the photoelectrochemical oxidation of $Et_2NCS_2^-$ to $[Et_2NC(S)S]_2$ at either illuminated CdS or CdSe. Oxidation of $Et_2NCS_2^-$ can be effected at an electrode potential significantly more negative than $E^{\circ\prime}$ of $Et_2NCS_2^-/[Et_2NC(S)S]_2$, showing that visible light can be used to drive the oxidation in an uphill sense. Compared to a Pt anode, the CdX (X = S, Se) photoanodes allow a voltage savings of the order of 1.0 V. The photoanodes are durable and show constant output of at least 10 mA/cm^2 for greater than 48 h.

In this article we show quantitative results relating to the strong interaction of sodium diethyldithiocarbamate, $Na[Et_2NCS_2]$ (I), disodium 1,2-ethanediylbis(ethyldithiocarbamate), $Na^+_2[CH_2N(Et)CS_2^-]_2$ (II), and disodium 1,6-hexanediylbis(methyldithiocarbamate), $Na^+_2[CH_2CH_2CH_2N(Me)CS_2^-]_2$ (III), with CdX (X = S, Se) electrode surfaces in CH_3CN/0.2 M $NaClO_4$ solution. The strong interaction of certain redox species with semiconductor electrodes has resulted in the demonstration of durable, efficient photoelectrochemical cells for the conversion of optical energy to electricity.[1] Two redox systems of importance are (1) X_n^{2-} (X = S, Se, Te), which interacts strongly with CdX semiconductors,[2] and (2) I_3^-/I^-, which interacts strongly with MoS_2 and related semiconductors.[3] The interaction of semiconductor surfaces with solution species can result in significant changes in the so-called flat-band potential, E_{FB}, of the semiconductor as shown in Scheme I for $CdS/Et_2NCS_2^-$. Excess negative charge on the surface is associated with a negative shift of E_{FB}.[4] In photoelectrochemical devices it is possible to exploit shifts in E_{FB} to realize greater photovoltages. An example is the n-type $MoS_2/I_3^-/I^-$ system where no photovoltage would be expected for the oxidation of I^- without the strong interaction of the redox couple leading to a negative shift of E_{FB}.[3] We have recently detailed the consequence of the interaction of RS^- with CdX (X = S, Se), with respect to shifts in E_{FB}.[5]

Scheme I. Representation of the Shift in E_{FB} of n-CdS upon Adsorption of $Et_2NCS_2^-$ in CH_3CN/0.2 M $NaClO_4$

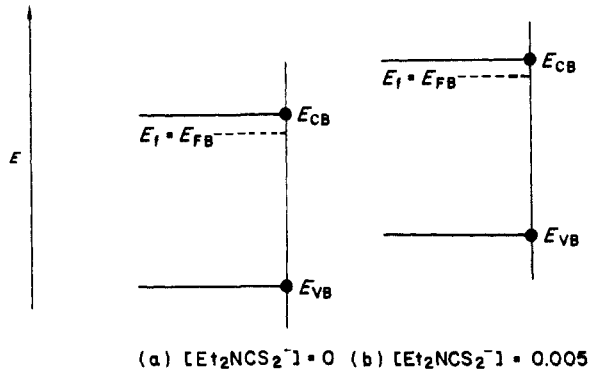

We now report that n-CdS and CdSe interact strongly with dithiocarbamates. The value of E_{FB} shifts in a direction such that light-driven oxidation according to eq 1 can be effected with a considerable voltage savings (about 1.0 V) compared to a conventional Pt anode known to effect the oxidation with unit current

$$2Et_2NCS_2^- + 2h^+ \rightarrow [Et_2NC(S)S]_2 \qquad (1)$$

(1) (a) Rajeshwar, K. *J. Appl. Electrochem.* **1985**, *15*, 1. (b) Nozik, A. J. *Annu. Rev. Phys. Chem.* **1978**, *23*, 1117.

(2) (a) Ellis, A. B.; Kaiser, S. W.; Wrighton, M. S. *J. Am. Chem. Soc.* **1976**, *98*, 1635. (b) Hodes, G.; Manassen, J.; Cahen, D. *Nature (London)* **1976**, *261*, 403. (c) Miller, B.; Heller, A. *Nature (London)* **1976**, *262*, 680.

(3) (a) Tributsch, H. *J. Electrochem. Soc.* **1978**, *125*, 1086. (b) Gobrecht, J.; Tributsch, H.; Gersicher, H. *J. Electrochem. Soc.* **1978**, *125*, 2085. (c) Turner, J. A.; Parkinson, B. A. *J. Electroanal. Chem.* **1983**, *150*, 611. (d) Fan, F.-R. F.; Bard, A. J. *J. Electrochem. Soc.* **1981**, *128*, 945. (e) Calabrese, G. S.; Wrighton, M. S. *J. Am. Chem. Soc.* **1981**, *103*, 6273.

(4) (a) Gerischer, H. In *Physical Chemistry: An Advanced Treatise*; Eyring, H., Henderson, D., Jost, W., Eds.; Academic: New York, 1970; Vol. 9A. (b) Bard, A. J.; Bocarsly, A. B.; Fan, F.-R. F.; Walton, E. G.; Wrighton, M. S. *J. Am. Chem. Soc.* **1980**, *102*, 3671.

(5) Natan, M. J.; Thackeray, J. W.; Wrighton, M. S. *J. Phys. Chem.*, in press.

0002-7863/86/1508-3570$01.50/0

efficiency.[6] The n-CdX/$Et_2NCS_2^-$ system illustrates a situation where strong interaction of the electroactive reagent leads to a high-efficiency photoelectrochemical oxidation from the standpoints of energy utilization and current efficiency.

Quantitative experiments show that equilibrium constant, K, for the process represented by eq 2 is such that the surface of CdX is at its maximum coverage of the $Et_2NCS_2^-$ when the solution

$$[CdX](s) + Et_2NCS_2^- \overset{K}{\rightleftharpoons} [CdX/^-S_2CNEt_2](s) \quad (2)$$

contains at least 5×10^{-3} M $Et_2NCS_2^-$, suggesting that large photovoltages can be maintained even at large-extent conversion in the oxidation process represented by eq 1, where the initial $Et_2NCS_2^-$ concentration can exceed 0.2 M. The interesting point is that the small $Et_2NCS_2^-$ concentration that remains at large-extent conversion of the initial sample is sufficient to maintain a negative value of E_{FB} to preserve high efficiency for optical energy utilization. The equilibrium constants for adsorption of I, II, and III vary considerably, and the rationale for the variations is discussed in terms of differences in bulk solubility and in molecular size.

Experimental Section

Electrode Preparation. Single crystals of low-resistivity (1 Ω-cm) n-CdS, cut perpendicular to the c axis, were obtained from Cleveland Crystals, Inc. The crystals were 1 mm thick and were cut into small pieces with a diamond-blade string saw. The crystals were etched in concentrated HCl for 30 s and rinsed with copious quantities of distilled H_2O prior to electrode fabrication. The shiny face of the polar (0001) crystal is Cd rich, and the dull face is S rich.[7] In all cases the cadmium-rich face has been exposed to electrolyte solution, due to its reproducibility in capacitance experiments and its equivalent performance in photoelectrochemical experiments. Ohmic contact from a layer of Ag epoxy on a flattened piece of Cu wire to the back of the crystal was made with a Ga–In eutectic mixture rubbed into the back of the CdS. The Cu wire was encased in 4-mm glass tubing, and the electrode was sealed with clear epoxy so that only the crystal remained exposed. Prior to any measurement or experiment, the electrodes were immersed in concentrated HCl, followed by 1.0 M Na_2S/1.0 M S/1.0 M NaOH solution, and distilled H_2O for 30 s each. The treatment with the polysulfide solution, followed by washing with H_2O, is needed to remove residual sulfur. Single crystals of low-resistivity (1 Ω-cm) n-CdSe were obtained from Cleveland Crystals, Inc. The n-CdSe electrodes were constructed and contacted in the same manner as n-CdS. The n-CdSe was etched with 3:1 HNO_3:HCl for 15 s, rinsed, immersed in 30% KCN for 2 min, and thoroughly rinsed prior to use. The donor density for both the CdS and the CdSe was determined to be 1.3×10^{17} cm^{-3} from the slopes of Mott–Schottky plots. Electrode areas exposed to the electrolyte solutions were in the range 0.05–0.10 cm^2.

Chemicals. $Na[Et_2NCS_2]\cdot 3H_2O$ and $[Et_2NC(S)S]_2$ were obtained from Aldrich; $NaClO_4$ (anhydrous) was obtained from G. Frederick Smith Chemicals. Diethylammonium diethyldithiocarbamate ($[Et_2NH_2][Et_2NCS_2]$) was purchased from Kodak Chemicals. All chemicals obtained commercially were used as received.

Disodium 1,2-ethanediylbis(ethyldithiocarbamate)·$4H_2O$ was prepared by using a slightly modified literature method.[8] Elemental analysis (Atlantic Microlabs) was satisfactory. Found $C_8H_{22}N_2O_4S_4Na_2$: (calcd) C, 25.68 (24.99); H, 5.36 (5.77); N, 7.35 (7.28); S, 33.66 (33.35). The ^1H NMR shows the expected splitting and integration (D_2O): 1.05 (t, 3 H), 3.05 (q, 2 H), 4.15 ppm (s, 2 H). Disodium 1,6-hexanediylbis(methyldithiocarbamate)·$2H_2O$ was synthesized according to a similar procedure. Elemental analysis (Atlantic Microlabs) was satisfactory. Found $C_{10}H_{22}N_2O_2S_4Na_2$: (calcd) C, 32.11 (31.90); H, 5.88 (5.89); N, 7.37 (7.44); S, 33.94 (34.05). The ^1H NMR in D_2O (integration) is as expected: 1.17 (m, 2 H), 1.53 (m, 2 H), 3.26 (s, 3 H), 3.87 ppm (t, 2 H).

Equipment. The reference electrode was a Ag/0.01 M $AgNO_3$/0.1 M $[(n\text{-}Bu)_4N]ClO_4/CH_3CN$ electrode, and the counterelectrode was a smooth Pt electrode of about 3-cm^2 area. Current–voltage data were obtained with a PAR Model 173 or ECO Model 551 potentiostat along with a PAR Model 175 programmer. The recorders used were either a Hewlett-Packard 7133A or Varian A-44 strip chart or a Houston Instruments Model 2000 X–Y. A digital coulometer was used to integrate the current vs. time.

Light sources for electrode illumination were a focused 200-W tungsten–halogen lamp, a beam-expanded Spectra Physics Model 164 Ar laser at 514 nm, or a beam-expanded He–Ne laser from Coherent Radiation at 632.8 nm. Light intensities were measured with a Tektronix J16 radiometer equipped with a J6502 probe and/or a calibrated Solarex Corporation photometer. The intensities were varied with a Variac variable-voltage source for the incandescent light, a photographic polarizing filter for the Ar laser, or a neutral density filter for the He–Ne laser.

Current–voltage curves were obtained at 5 mV/s for stirred N_2-purged electrolyte solutions. Controlled-potential electrolyses were performed under N_2 in two-compartment cells separated by a medium or fine glass frit. The anolyte was well stirred in all experiments.

HPLC Analysis. High-pressure liquid chromatography (HPLC) was accomplished with a Hewlett-Packard 1084b chromatograph, with detection from 190 to 600 nm at a rapid-scan UV–vis detector. Peaks were monitored at 254 nm, and the UV–vis spectrum was obtained for the species associated with the peaks. For a $Et_2NCS_2^-/[Et_2NC(S)S]_2$ separation, a mobile phase gradient of 65% MeOH/H_2O to 90% MeOH/H_2O over 10 min can be used. The stationary phase was a Hewlett-Packard RP-8 reversed-phase 5-μm column (250 mm × 4.6 mm i.d.). The entire pumping system was kept under Ar to prevent air (O_2) oxidation of injected samples.

Differential Capacitance Measurements. The differential capacitance of n-CdS and n-CdSe was measured under Ar in the dark, employing a PAR Model 5204 lock-in Amplifier with an internal oscillator. A 5-mA peak-to-peak sine wave, from 1 to 10 kHz, was used as the AC modulation. The DC bias was provided by the PAR Model 173 potentiostat. Capacitance values were extracted from the quadrature values by assuming a simple resistance–capacitance circuit. A dummy resistance–capacitance circuit was used to calibrate the measurement system. Quadrature values were insensitive to resistance over the range 100–1000 Ω, indicating a strict proportionality of the quadrature output to the actual capacitance data.

Auger Spectroscopy. Auger electron spectra were obtained with a Physical Electronics Model 590A scanning Auger spectrometer. A 5-keV electron beam with a beam current of 0.1–1 μA was used as the excitation source. Elements detected by Auger were identified by reference to data previously reported with this technique.[9]

Results and Discussion

Photoelectrochemical Oxidation of Sodium Diethyldithiocarbamate at n-CdX (X = S, Se). The oxidative coupling of dithiocarbamates to form the corresponding dithiuram disulfide at an electrode is an important commercial process.[10] We have shown quantitatively that $Et_2NCS_2^-$ can be oxidized to $[Et_2NC(S)S]_2$, eq 1, with unit current efficiency. Figure 1 shows a typical steady-state photocurrent–voltage curve for both n-CdS and n-CdSe in a 0.1 M $Na[Et_2NCS_2]$/0.1 M $NaClO_4/CH_3CN$ electrolyte. We have chosen CH_3CN as the solvent because the dithiocarbamate and disulfide are both soluble in this medium. In H_2O the initial photocurrent–voltage curve looks virtually the same as in CH_3CN, Figure 1, but a precipitate of the disulfide rapidly builds up on the electrode surface, leading to a decline in photocurrent. In CH_3CN, we have achieved photoanodic current onsets at potentials of −1.77 V vs. Ag/Ag^+ for n-CdS and −1.59 V vs. Ag/Ag^+ for n-CdSe photoanodes. Based on the $E^{\circ\prime}$ for the $[Et_2NC(S)S]_2/EtNCS_2^-$ redox couple of −0.605 V vs. Ag/Ag^+,[11] we find 1.2 and 1.0 V of voltage savings at n-CdS and n-CdSe, respectively. Other workers have achieved unit current efficiency oxidations at Pt electrodes.[6]

The insets of Figure 1 show a measure of the durability of the n-CdX photoanodes over extended periods of time. There is virtually no change in the photocurrent density at n-CdX over a 72-h period at photocurrent densities of the order of 10 mA/cm^2. It is worth noting that the photocurrent–voltage curves do not change appreciably, even after consumption of 70% of the starting dithiocarbamate. Auger spectroscopy shows that the CdSe

(6) Cauquis, G.; Lachenal, D. *J. Electroanal. Chem.* **1973**, *43*, 205.
(7) Warekois, E. P.; Lavine, M. C.; Mariano, A. N.; Gatos, H. C. *J. Appl. Phys.* **1962**, *33*, 690.
(8) (a) Clifford, A. M.; Lichty, J. G. *J. Am. Chem. Soc.* **1932**, *54*, 1163. (b) Ivin, K. J.; Lillie, E. D. *Makromol. Chem.* **1978**, *179*, 591.
(9) Davis, L. E.; MacDonald, N. C.; Palmberg, P. W.; Riach, G. E.; Weber, R. E. *Handbook of Auger Electron Spectroscopy*, 2nd ed.; Physical Electronics Division, Perkin-Elmer Corporation: Eden Prairie, Minnesota, 1967.
(10) Jansson, R. *Chem. Eng. News* **1984**, *62*(47), 43.
(11) Nichols, P. J.; Grant, M. W. *Aust. J. Chem.* **1982**, *35*, 2455.

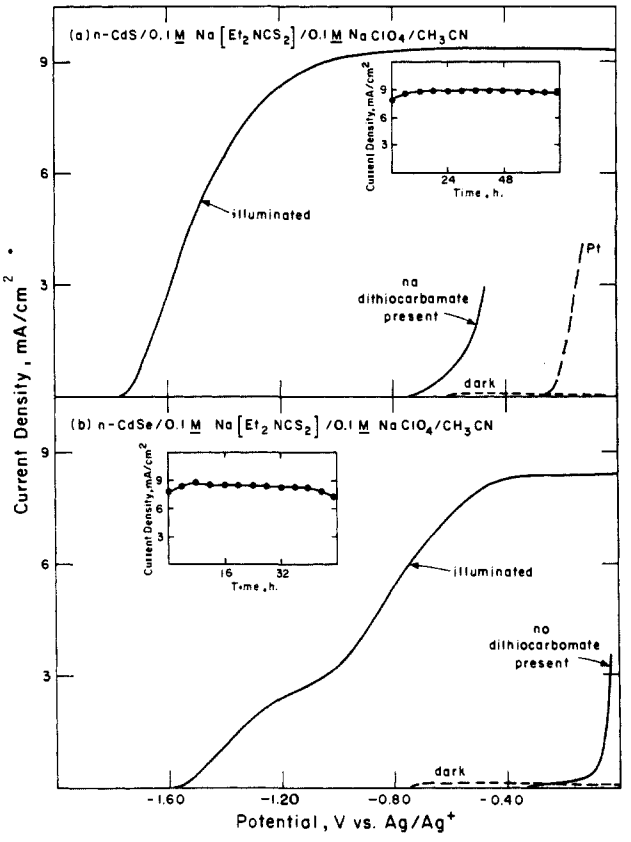

Figure 1. Steady-state photocurrent–voltage curves for 0.1 M Na-$[Et_2NCS_2]$ in 0.1 M $NaClO_4/CH_3CN$ at (a) n-CdS and (b) n-CdSe under white light illumination (about 80 mW/cm^2). The insets show the plots of photocurrent density vs. time for these electrodes.

electrode does not extract S from the dithiocarbamate or its oxidation product. Figure 2 shows a comparison of the Auger spectra of a freshly etched CdSe surface, a CdSe electrode dipped into a CH_3CN solution of $Na[Et_2NCS_2]$, and a CdSe surface used for a prolonged photoelectrochemical oxidation of $Et_2NCS_2^-$. The presence of S from $Et_2NCS_2^-$ adsorbed onto the CdSe is consistent with its slow desorption from the surface, but there is no evidence for S buildup on the electrode used for a prolonged photoelectrochemical oxidation.

It is also apparent from Figure 1 that the photoelectrochemical oxidation of $Et_2NCS_2^-$ proceeds far more efficiently at n-CdS than at n-CdSe. The steady-state photocurrent–voltage curve for CdSe shows relatively poor rectangularity, and the shape of the curve in the negative potential region suggests poor kinetics for product formation, or low rates of product desorption resulting in overall poor kinetics, at negative potentials. We have attempted a number of different etching procedures for n-CdSe in order to improve the steady-state photocurrent–voltage curve without success.

Essentially unit current efficiency for the photoelectrochemical oxidation of $Et_2NCS_2^-$ at illuminated CdX electrodes has been established by monitoring product formation as a function of charge passed. Figure 3 shows results from a typical experiment where we determined the current efficiency for the photoelectrochemical oxidation of $Na[Et_2NCS_2]$ at n-CdSe. Utilizing high-pressure liquid chromatography (HPLC), we have achieved excellent separation and resolution of the dithiocarbamate from its corresponding disulfide. In the figure, the peak for the $[Et_2NC(S)S]_2$ grows in, while the $Et_2NCS_2^-$ peak decreases. The rapid-scan UV spectra for the starting material and product peak in the HPLC traces shown in Figure 3 are the same as those obtained for authentic samples of the starting material and product in the same medium. Thus, the detector of the HPLC allows identification of product both on the basis of retention time and on the basis of UV spectral features. In Table I the current efficiencies at various points in the electrolysis are given and data for photoelectrochemical oxidation at n-CdS are included. For

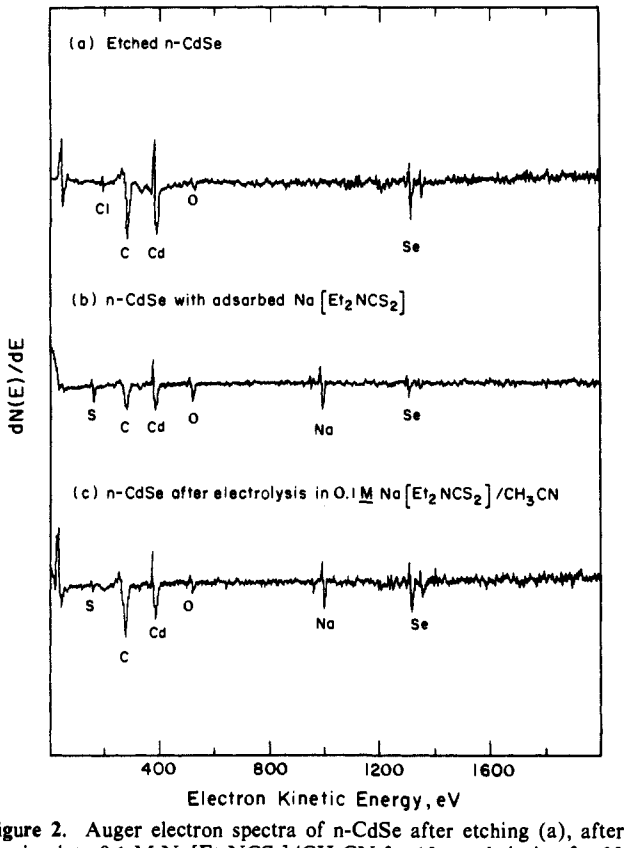

Figure 2. Auger electron spectra of n-CdSe after etching (a), after dipping into 0.1 M $Na[Et_2NCS_2]/CH_3CN$ for 10 s and rinsing for 30 s with CH_3CN (b), and after use in the photoelectrochemical oxidation of $Et_2NCS_2^-$ for more than 70 h as in Figure 1 (c).

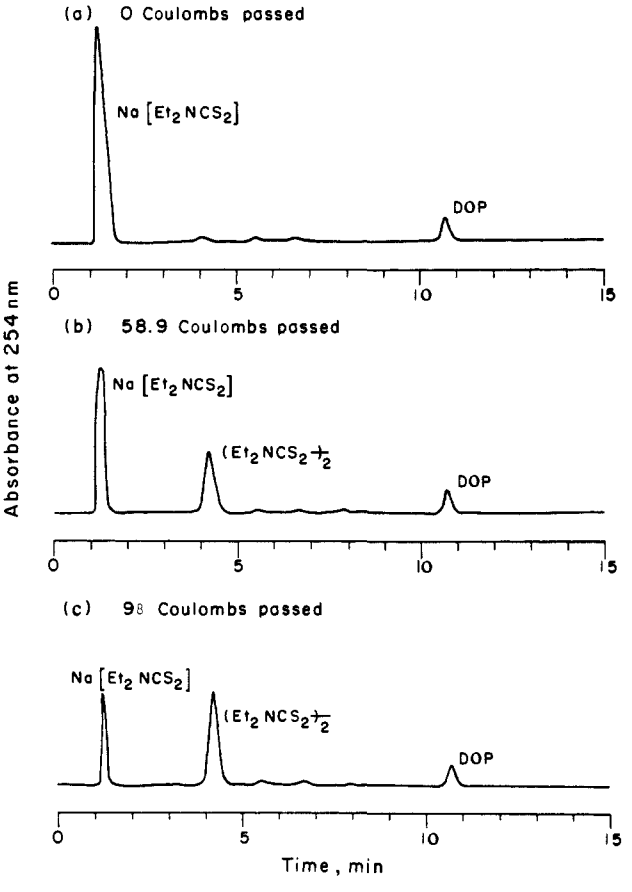

Figure 3. High-pressure liquid chromatograms vs. charge passed during a controlled-potential electrolysis of $Na[Et_2NCS_2]/0.1$ M $NaClO_4/CH_3CN$. Conditions are as described in Figure 1. DOP, dioctyl phthalate, is an internal standard.

Table I. Current Efficiency Experiments for the Photoelectrochemical Oxidation of 0.1 M $Na[Et_2NCS_2]$/0.1 M $NaClO_4/CH_3CN$ at n-CdSe and n-CdS

electrode[a]	potential vs. Ag/Ag^+, V	% convn (C)	current eff.[b]	savings vs. Pt,[c] V
n-CdSe	−0.70[d]	24.5	100%	0.8
		(34.4)		
		42	99%	
		(58.9)		
		70	98%	
		(98.5)		
n-CdS	−1.00[e]	26.5	99%	1.1
		(42.5)		
		50.4	98%	
		(80.9)		
		65	99%	
		(104)		

[a] The electrodes (0.05–0.1 cm^2) were illuminated with a tungsten-halogen lamp at 80 mW/cm^2. The current density was about 10 mA/cm^2. [b] The current efficiencies were determined by measuring the amount of disulfide formed over time by HPLC (see Experimental Section) and directly comparing it to the amount of charge passed. [c] The potential difference between n-CdX and Pt for the same current density defines the voltage savings. [d] The current density for this experiment was 9 mA/cm^2 at −0.70 V vs. Ag/Ag^+. [e] The current density for this experiment was 10 mA/cm^2 at −1.00 V vs. Ag/Ag^+.

both n-CdS and n-CdSe, the current efficiency for the oxidation at all points is 99 ± 2%. Thus, at n-CdS and n-CdSe, the sole oxidation process is given by eq 1. In both cases, we have gone to large-extent conversions in order to show that CdS and CdSe photoelectrodes still perform efficiently even when the dithiocarbamate is substantially depleted. The unit current efficiency, the large-extent conversion, and the large photocurrent densities that are seen at these photoanodes make them ideal candidates for the photoelectrochemical generation of dithiuram disulfides.

Output Parameters at n-CdX for the 0.1 M $Na[Et_2NCS_2]$/0.01 M $[Et_2NC(S)S]_2$/0.1 M $NaClO_4/CH_3CN$ Electrolyte System. We have generated steady-state photocurrent–voltage curves at n-CdX (X = S, Se) for the 0.1 M $Na[Et_2NCS_2]$/0.01 M $[Et_2NC(S)S]_2$/0.1 M $NaClO_4/CH_3CN$ system with 514.5-nm input optical power. The maximum power conversion efficiency, η_{max}, is given by eq 3, where i is the photocurrent and E_v is the photovoltage.

$$\eta_{max} = [(iE_v)_{max}/\text{optical power}] \times 100\% \quad (3)$$

$$FF = [(iE_v)_{max}/(E_{v(oc)}i_{sc})] \quad (4)$$

The fill factor, a measure of the rectangularity of the photocurrent–voltage curves, is given by eq 4, where i_{sc} is the photocurrent at E_{redox} and $E_{v(oc)}$ is the open-circuit photovoltage. Output parameters associated with the photocurrent–voltage curves are given in Table II. Although the photooxidation of $Et_2NCS_2^-$ is irreversible (in the sense that there is not a good electrode for the reverse process), the calculation of the output parameters provides a useful means for illustrating the theoretical power savings that can be realized in a photoelectrochemical synthesis of $[Et_2NC(S)S]_2$. In the determination of the output parameters, the value of E_{redox} is based on the $E^{\circ\prime}$ for the $Et_2NCS_2^-/[Et_2NC(S)S]_2$ couple of −0.605 V vs. Ag/Ag^+.[11] At n-CdS, we obtain an $E_{v(oc)}$ greater than 1.0 V, with a maximum of 1.14 V, almost half the band gap of n-CdS. These are among the largest photovoltages ever obtained at n-CdS and certainly provide evidence of the strong interaction of $Et_2NCS_2^-$ with n-CdS, because the value of E_{FB} in the absence of a strong interaction would suggest much smaller photovoltages, vide infra. At least for CdS, the large photovoltages are accompanied by excellent fill factors and high η_{max}, with FF = 0.55 and η_{max} = 20.9% at 10 mW/cm^2 (514.5-nm light). The relatively low solubility of $Na[Et_2NCS_2]$ (about 0.2 M) in CH_3CN can be circumvented by using $[Et_2NH_2][Et_2NCS_2]$, which has a solubility of about 1.0 M in CH_3CN. In a 1.0 M $[Et_2NH_2][Et_2NCS_2]$/0.01 M $[Et_2NC(S)S]_2$/0.2 M $[(n\text{-}Bu)_4N]ClO_4/CH_3CN$ electrolyte, we obtain η_{max} = 15.3% and FF = 0.44 at 60 mW/cm^2 (514.5-nm light). This system may be a good candidate for nonaqueous, n-CdS-based photoelectrochemical cells for the conversion of light to electricity, provided that a good counterelectrode can be found to reduce the $[Et_2NC(S)S]_2$. All the output parameters for n-CdSe are less than those for n-CdS, presumably stemming from the difficulties associated with the interface noted above in discussing the shape of the photocurrent–voltage curves.

Table II. Output Parameters at n-CdS and n-CdSe in 0.1 M $Na[Et_2NCS_2]$/0.01 M $[Et_2NC(S)S]_2$/0.1 M $NaClO_4/CH_3CN$ Solution

electrode	input optical power,[a] mW/cm^2	Φ_e[b]	η_{max}[c]	FF[d]	$E_{v(oc)}$,[e] V
n-CdS	3.22	0.77	20.7%	0.63	1.03
	10.00	0.84	20.9%	0.55	1.09
	32.25	0.78	16.2%	0.44	1.14
n-CdSe	3.22	0.82	8.0%	0.30	0.64
	10.00	0.79	6.2%	0.21	0.72
	32.90	0.69	3.7%	0.16	0.73

[a] Input power is at 514.5 nm for CdS and 632.8 nm for CdSe. [b] Quantum yield for electron flow at E_{redox}. Data are uncorrected for reflection losses. [c] η_{max}, % is defined in eq 3. [d] Fill factor is defined in eq 4. [e] $E_{v(oc)}$ is the difference in potential for the onset of photocurrent and E_{redox}.

Measurement of Flat-Band Shifts by Capacitance. The flat-band potential of a semiconductor electrode, E_{FB}, depends on the amount of excess charge, Q_{ads}, on the surface due to adsorbed charged species. When there are charged species adsorbed on the semiconductor there is a voltage drop across the Helmholtz layer, E_H, which is the magnitude of the shift in E_{FB} of the semiconductor from its value in an innocent (noninteracting) electrolyte solution.[12] Changes in E_{FB} upon variation in solution concentration of the adsorbing species are then equal to the changes in the Helmholtz voltage by charged adsorbate. It is assumed that the Helmholtz capacity, C_H, given by eq 5, is constant.[12,13] Observed shifts in

$$C_H = Q_{ads}/E_H \quad (5)$$

E_{FB} are then a direct measure of the extent of strong adsorption of charged species from the electrolyte.

The technique of differential capacitance is a way to obtain values of E_{FB}.[12] The capacitance of an ideal semiconductor/electrolyte junction should obey the Mott–Schottky relation, eq 6, at values of E_f where a depletion layer is formed. In eq 6, n

$$[C_{sc}]^{-2} = 2[-(E_f - E_{FB}) - kT/e]/n\epsilon\epsilon_0 e \quad (6)$$

is the donor density, ϵ is the semiconductor dielectric constant, ϵ_0 is the permittivity of free space, and e is the electronic charge.[14] The literature values for ϵ are 5.4 and 10 for n-CdS and n-CdSe, respectively.[15] In the absence of a high density of surface states or deep donor levels, a plot of $1/C_{sc}^2$ vs. E_f should be linear and have an extrapolated intercept equal to E_{FB} (the correction for kT/e equals 27 mV at room temperature). We have observed ideal Mott–Schottky behavior at frequencies of 1–10 kHz and find the differential capacitance measured to be solely due to the capacity of the space charge layer of the semiconductor.

Figure 4 shows Mott–Schottky plots for CdX in the presence of various $Et_2NCS_2^-$ concentrations. The plots for a given semiconductor electrode are linear and parallel and give increasingly negative values of E_{FB} with addition of $Et_2NCS_2^-$ to the solution. Since the $Na[Et_2NCS_2]$ contains a small quantity of $[Et_2NC(S)S]_2$ (see Figure 3, less than 1%), the value of E_{redox} is defined for these measurements. However, the $[Et_2NC(S)S]_2$ has no bearing on E_{FB}, as addition of pure $[Et_2NC(S)S]_2$ to a 0.1 M $NaClO_4$ solution induces no shift of E_{FB}, and the capacitance–voltage curves recorded for solutions containing $Et_2NCS_2^-$ are not

(12) Morrison, S. R. *Electrochemistry at Semiconductor and Oxidized Metal Electrodes*; Plenum: New York, 1980, pp 49–142.
(13) Frese, K. W., Jr.; Canfield, D. G. *J. Electrochem. Soc.* **1984**, *131*, 2614.
(14) Myamlin, V. A.; Pleskov, Y. V. *Electrochemistry of Semiconductors*; Plenum: New York, 1967.
(15) Sze, S. M. *Physics of Semiconductor Devices*; Wiley: New York, 1981.

Table III. Flat-Band Potentials and Derived Values of Surface Coverage, θ, of $Et_2NCS_2^-$ on n-CdS[a]

$[Et_2NCS_2^-]$, M	E_{FB}(V vs. Ag/Ag$^+$) ± 50 mV[b]	θ
0	−0.80	0
0.0001	−0.90	0.10
0.0002	−0.96	0.17
0.0003	−0.99	0.19
0.0004	−1.055	0.27
0.0005	−1.12	0.33
0.0006	−1.18	0.39
0.0007	−1.23	0.44
0.0008	−1.32	0.53
0.0009	−1.37	0.58
0.0010	−1.42	0.62
0.002	−1.49	0.69
0.0025	−1.59	0.80
0.004	−1.683	0.89
0.006	−1.72	0.93
0.008	−1.725	0.93
0.200	−1.79 (E_{FB}^{sat})	1.0

[a] The electrolyte solution was 0.2 M $NaClO_4/CH_3CN$; all measurements were made in the dark (see Experimental Section). [b] Differences in E_{FB} have an estimated error of 10 mV.

Table IV. Flat-Band Potentials and Derived Values of Surface Coverage, θ, of $Et_2NCS_2^-$ on n-CdSe[a]

$[Et_2NCS_2^-]$, M	E_{FB}(V vs. Ag/Ag$^+$) ± 50 mV[b]	θ
0	−0.60	0
0.0001	−0.72	0.13
0.0002	−0.77	0.18
0.0004	−0.89	0.30
0.0006	−0.94	0.36
0.0012	−1.01	0.43
0.0025	−1.24	0.67
0.00275	−1.29	0.73
0.003	−1.35	0.79
0.004	−1.42	0.86
0.005	−1.45	0.90
0.007	−1.46	0.91
0.200	−1.55 (E_{FB}^{sat})	1.0

[a] The electrolyte solution was 0.2 M $NaClO_4/CH_3CN$; all measurements were made in the dark (see Experimental Section). [b] Differences in E_{FB} have an estimated error of 10 mV.

altered by the presence of the $[Et_2NC(S)S]_2$. The changes in E_{FB} are independent of the frequency of the AC signal in the range 1 kHz to 10 kHz. Tables III and IV show values of E_{FB} vs. concentration of $Na[Et_2NCS_2]$ for n-CdS and n-CdSe, respectively. We note that the most negative E_{FB} values, E_{FB}^{sat}, are −1.79 and −1.55 V vs. Ag/Ag$^+$ at n-CdS and n-CdSe, respectively. These values correspond very well with the potentials for the onset of photoanodic current, Figure 1. At the other extreme, in the absence of $Na[Et_2NCS_2]$, the values of E_{FB} vs. Ag/Ag$^+$, are −0.80 V for n-CdS, and −0.60 V for n-CdSe, approximately 400 mV positive of those reported for these electrodes in aqueous electrolytes.[16] The same electrodes giving these values in CH_3CN/0.1 M $NaClO_4$ showed the expected values for E_{FB} in aqueous solutions.[16] One final point that should be made concerning the Mott–Schottky plots and the associated values of E_{FB} is that $Et_2NCS_2^-$ appears to only slowly desorb from the CdX surface. The Auger spectroscopy in Figure 2 illustrates that adsorbed $Et_2NCS_2^-$ can be detected even after the surface is rinsed thoroughly with pure CH_3CN. Additionally, if the E_{FB} value is determined in 0.1 M $Na[Et_2NCS_2]$/0.1 M $NaClO_4$ and the electrode is then moved to a solution free of the adsorbing anion the E_{FB} only slowly, on the time scale of a few minutes, moves to a more positive value of E_{FB}. In contrast, when a CdX electrode is immersed in the solution containing the adsorbing anion, the E_{FB} value is quickly established to be its equilibrium value.

As discussed earlier, shifts in E_{FB} are attributed to the potential drop across the Helmholtz layer, E_H, brought about by strong

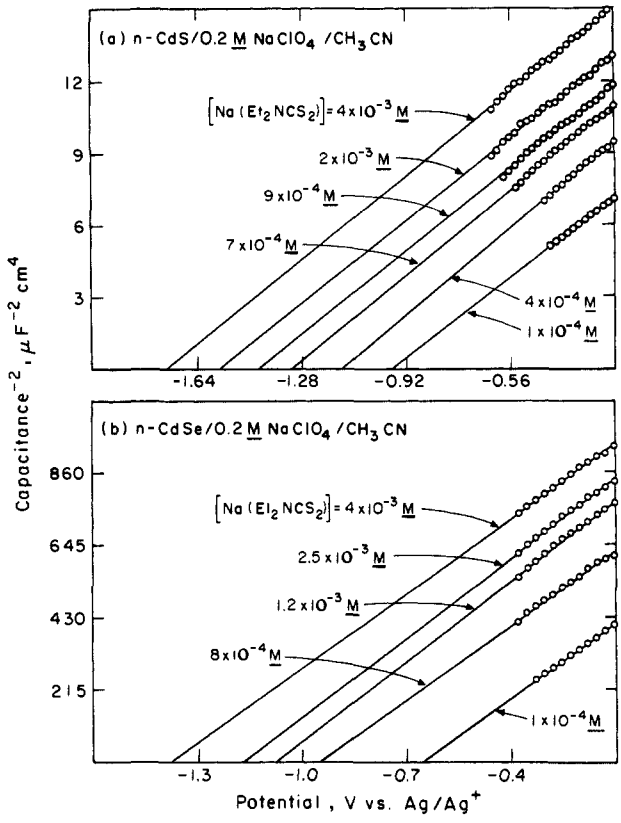

Figure 4. Plots of $1/C_{sc}^2$ vs. electrode potential, E_f, for various concentrations of $Na[Et_2NCS_2]$.

adsorption of charged species. From the negative direction of the shifts in E_{FB}, it follows that the $Et_2NCS_2^-$ anion is the adsorbing species. From Figure 4, and from Tables III and IV, it is apparent that Q_{ads}, and therefore the concentration of adsorbed $Et_2NCS_2^-$, increases with increasing solution concentration. Adsorption isotherms relate surface concentrations to solution concentrations, and we have compared our experimentally derived adsorption isotherms to the Langmuir model and, to a first approximation, find excellent agreement, as developed below.

Absorption Isotherms and Comparison with the Langmuir Model. Adsorption isotherms, plots of fractional surface coverage vs. solution concentration, can be constructed from the data in Tables III and IV by use of eq 7, as developed in ref 13. $E_{FB}°$ is the

$$\theta = (E_{FB} - E_{FB}°)/(E_{FB}^{sat} - E_{FB}°) \quad (7)$$

flat-band potential in the absence of adsorbing species and E_{FB}^{sat} is the most negative value of E_{FB} (at the maximum coverage of adsorbed negative species). Here θ is defined in the usual sense, referring to the fractional surface coverage of the adsorbed species, and can vary from 0 to 1. E_{FB}^{sat} is associated with the maximum coverage attainable at a given temperature in a given solvent.

There exist two treatments of semiconductor/liquid junctions relating the concentration of adsorbed species to thermodynamic parameters and the bulk solution activity, A_x: Morrison considers the free energy of adsorption to vary linearly with E_H, a solely electrostatic view of the adsorption process;[12] Frese considers the equilibrium constant for adsorption, a purely chemical contribution, without regard to the Helmholtz potential dependence of adsorption.[13] Adamson points out[17] that both terms can be important and writes as a general relationship eq 8, where A_x is the

$$\theta/(1 - \theta) = A_x(\exp[(zeE_H + \Phi)/kT]) \quad (8)$$

solution activity of the adsorbing species, z is the charge of the adsorbed species, e is the charge of an electron, and Φ refers to chemical potential contributions. This equation places the Stern

(16) Ellis, A. B.; Kaiser, S. W.; Bolts, J. M.; Wrighton, M. S. *J. Am. Chem. Soc.* **1977**, *99*, 2839.

(17) Adamson, A. *Physical Chemistry of Surfaces*; Wiley: New York, 1982; pp 185–231, 369–401.

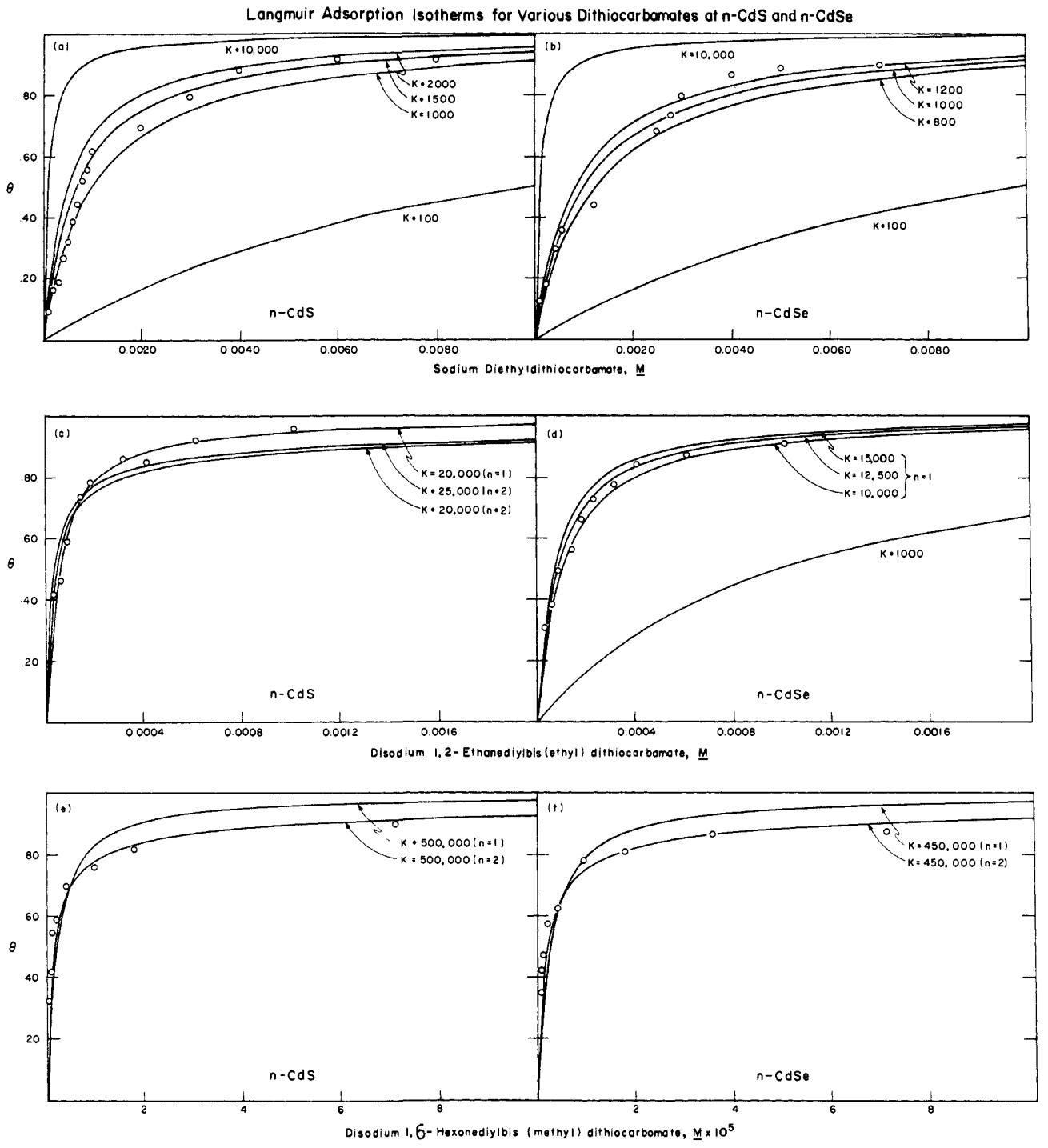

Figure 5. Langmuir adsorption isotherms at n-CdS and n-CdSe derived from E_{FB} data for (a, b) $Et_2NCS_2^-$, (c, d) $[CH_2N(Et)CS_2^-]_2$, (e, f) $[(CH_2)_3N(Me)CS_2^-]_2$.

equation in a form more suited to Langmuir-type behavior.[17] Here both electrostatic and chemical contributions to the free energy of adsorption are considered. In Frese's treatment, the zeE_H term is set equal to zero, and $\Phi = -(f\theta + \Delta G)$, where f is the parameter characterizing the interaction between adsorbing species (the Frumkin isotherm)[18] and ΔG represents the change in free energy for the adsorption reaction. In Morrison's treatment, the chemical potential term $\Phi = 0$ and $\theta/1 - \theta$ has been replaced by $B\theta$, where B is a constant (the Henry isotherm).[17] We have compared our isotherms to those derived from the simplest model for adsorption, the Langmuir isotherm, which assumes no interaction between adsorbed species. This can be considered a special case of the Frumkin isotherm, where $f = 0$. We, too, neglect the potential dependence of adsorption but find that we get reasonable fits of our data using the Langmuir equation, eq 9, where K is the

$$\theta/(1 - \theta) = Kc \qquad (9)$$

equilibrium constant for the reaction in eq 2 and c is the solution concentration, assumed to be a good approximation to A_x at concentrations of less than 5 mM. Others have used Langmuir isotherms in explaining behavior of semiconductors in the presence of charged, adsorbing molecules.[19]

Figure 5 shows the experimental adsorption isotherms for three dithiocarbamates, species I–III, at both n-CdS and n-CdSe. For

(18) Gileadi, A., Ed. *Electrosorption*; Plenum: New York, 1967, pp 1–52.

(19) (a) Rossetti, R.; Beck, S. M.; Brus, L. E. *J. Am. Chem. Soc.* **1984**, *106*, 980. (b) Herrmann, J.; Pichat, P. *J. Chem. Soc., Faraday Trans. 1* **1980**, *76*, 1138.

all three species the Mott–Schottky plots from which the values of E_{FB} have been determined are linear and have the same slope (for a given electrode), and as the concentration of adsorbate is changed the Mott–Schottky plots are parallel to each other. In short, the data used to generate the adsorption isotherms in Figure 5 are as good as the data shown in Figure 4 for $Et_2NCS_2^-$. In each case, we have plotted, for comparison, isotherms for perfect Langmuir behavior, neglecting any potential dependence for adsorption and taking $f = 0$. We have varied K such that the hypothetical isotherms closely fit the observed data. Figure 5 shows plots of θ vs. concentration for $Na[Et_2NCS_2]$ at n-CdS and n-CdSe. Clearly, an equilibrium constant of 100 or 10 000 M^{-1} does not fit the experimental data for either semiconductor. The curves for n-CdS and CdSe indicate equilibrium constants of 2000 and 1000 M^{-1}, respectively, assuming the Langmuir equation.

Several important features of the adsorption of $Et_2NCS_2^-$ are indicated in Figure 5. First, the Langmuir model gives a surprisingly reasonable fit to the data, better than can be obtained with the Frumkin model with any single, nonzero value of f. Of course, it must be noted that f could be a function of θ,[13] which would add unnecessary complication to the analysis. This is to be contrasted with the adsorption of OH^- and S^{2-} from aqueous solutions onto n-CdSe, where strong interaction between adsorbed species is observed.[13] The close fit to Langmuir behavior found for the dithiocarbamates on n-CdX indicates that for this particular system, the Helmholtz potential (E_H) dependence of the adsorption process can be ignored in the electrode potential (E_f) range investigated. The second feature of importance is that the surfaces of the semiconductors are both close to their saturation coverage (θ greater than 0.9) in the presence of 4 mM $Et_2NCS_2^-$, a result that correlates well with the good photoelectrochemical output parameters at large-extent conversions of 0.1 M $Et_2NCS_2^-$ solutions. The third feature of importance is that $Et_2NCS_2^-$ seems to slightly favor the CdS binding sites compared to the CdSe sites, as evidenced by the difference in the equilibrium constants for the two semiconductors.

Structure variation of the dithiocarbamate has interesting consequences on the shifts in E_{FB}. Figure 5 includes adsorption isotherms for a structural analogue of $Et_2NCS_2^-$, $-[CH_2N(Et)CS_2^-]_2$ (II), a molecule with two dithiocarbamate functionalities but with the same types of alkyl groups on the nitrogens. The adsorption of this molecule fits ideal Langmuir isotherms extremely well. Adsorption of a species from the electrolyte solution likely involves the replacement of at least one surface-bound solvent molecule, and, in this case, the possibility of displacing several molecules of CH_3CN exists with each molecule of II adsorbed onto the semiconductor surface. The Langmuir relation for the case of two solvent molecules displaced ($n = 2$)[18] is shown in eq 10. The adsorption isotherm for $n = 2$ rises more steeply and

$$\theta = 1 - (4Kc + 1)^{-1/2} \quad (10)$$

levels off more quickly than the isotherm for single solvent molecule displacement ($n = 1$) that has been assumed for $Et_2NCS_2^-$ adsorption. The experimental data in Figure 5c give a better fit to the single molecule displacement isotherm, giving $K = 20\,000\ M^{-1}$. For n-CdSe, the $n = 1$ model is again best, giving $K = 12\,500\ M^{-1}$. Again, the equilibrium constant for n-CdS is greater than for n-CdSe, but there are important differences in the behavior of I and II, with respect to adsorption. For II near saturation coverage of the surface occurs at 500 μM, a factor of 10 lower than is necessary for I. Also, the absolute magnitudes of the shifts in E_{FB} are much lower for II than for I, only 290 mV for n-CdS and 420 mV for n-CdSe. Evidently, the saturation coverage for II is lower than for I. This is not an unreasonable finding considering the difference in the sizes of the two species.

Finally, Figure 5 includes experimental and theoretical adsorption isotherms at n-CdS and n-CdSe for III, a bis(dithiocarbamate) with the $-CS_2^-$ groups separated by a six-carbon chain. The data fit an adsorption isotherm derived from eq 10 with $n = 2$, suggesting the displacement of two molecules of solvent per molecule of III adsorbed. The best fit gives equilibrium constants of $5 \times 10^5\ M^{-1}$ and $4.5 \times 10^5\ M^{-1}$ for n-CdS and n-CdSe, respectively. Nearly complete saturation adsorption of the surface of the semiconductors with III occurs at approximately 20 μM. The maximum shifts in E_{FB} from adsorption of III are only 170 mV for n-CdS and 310 mV for n-CdSe. Again, we conclude that such a result signals that the adsorbing molecule, III, yields a smaller maximum coverage than I.

Table V. Values of $(E_{fb}^{sat} - E_{fb}°)$, K, and n for Different Dithiocarbamates at n-CdS and n-CdSe

dithiocarbamate	$(E_{FB}^{sat} - E_{FB}°)$, V	K, M^{-1}	n
n-CdS			
$Na[Et_2NCS_2]$ (I)	0.99	2×10^3	1
$Na^+_2[CH_2N(Et)CS_2^-]_2$ (II)	0.29	2×10^4	1
$Na^+_2[(CH_2)_3N(Me)CS_2^-]_2$ (III)	0.17	5×10^5	2
n-CdSe			
$Na[Et_2NCS_2]$ (I)	0.95	1×10^3	1
$Na^+_2[CH_2N(Et)CS_2^-]_2$ (II)	0.42	1.2×10^4	1
$Na^+_2[(CH_2)_3N(Me)CS_2^-]_2$ (III)	0.31	4.5×10^5	2

Table V summarizes the values of $E_{FB}^{sat} - E_{FB}°$, K, and n for I–III adsorption onto CdS and CdSe. The quantity, $E_{FB}^{sat} - E_{FB}°$, the maximum Helmholtz voltage, and therefore the maximum shift of E_{FB}, provide measures of the relative surface coverage of the specifically adsorbing ions I–III. For these moelcules, $E_{FB}^{sat} - E_{FB}°$ increases in the order III < II < I. This ordering correlates with the size of the molecules; that is, larger dithiocarbamates give smaller surface coverage, thus leading to smaller shifts in E_{FB}. The same ordering of coverage of I–III is found at n-CdS and n-CdSe.

The equilibrium constant for adsorption, K, increases in the order I < II < III for both CdS and CdSe. For this ordering, the relative ratio of K is 1:10:250. We thus find an equilibrium constant for III 250 times greater than that for I. A major contributing factor to the observed variation in K is the variation in solubilities of the dithiocarbamates. The solubility of these molecules in CH_3CN is about 0.20 M for $Na[Et_2NCS_2]$, about 0.020 M for $Na^+_2[CH_2N(Et)CS_2^-]_2$, and about 0.0056 M for $Na^+_2[CH_2CH_2CH_2N(Me)CS_2^-]_2$. The solubility ratio of I:II:III is thus 36:3.6:1, showing that the largest K is associated with the least soluble dithiocarbamate. It is known that bulk solubility is inversely proportional to the adsorbability.[18]

Interestingly, the value of K is larger for CdS than for CdSe, but for the two firmly bound species, II and III, the shift of E_{FB} is larger for CdSe than for CdS. The stronger binding of the anions to CdS should not be overinterpreted; the equilibrium constants are systematically larger for CdS, but the diffeence in K is not more than a factor of 2. The greater shift of E_{FB} for adsorption of II and III on CdSe may be a fundamental result, but again the effect is difficult to interpret and stems from less than a factor of 2 variation in coverage for a given adsorbate. It is tempting to conclude that both the systematic trend in K and the E_{FB} shift with CdS vs. CdSe is a reflection of the nature of the semiconductor/adsorbate interaction, but it is important to note that differences in the surfaces may arise from the differences in the surface morphology due to different surface pretreatments.

The number of solvent molecules displaced, n, in the best fit, by the adsorbing molecule is given in Table V. Only the largest molecule, III, gives a good fit to a Langmuir adsorption isotherm for a two-solvent-molecule displacement. It is not possible to determine whether the chelate effect or the long alkyl chain is responsible for the second solvent molecule displacement. All three molecules studied in CH_3CN fit a Langmuir adsorption isotherm, and the adsorption data accord well with the electrochemical observables for I. Detailed electrochemical studies of II and III have not been carried out, because the low solubility of II and III precludes efficient photoelectrochemical performance at high light intensities.

Estimation of Saturation Coverage of Adsorbates. The Langmuir adsorption isotherm model assumes monolayer coverage, and since the Helmholtz layer is generally accepted to be about (3–5) $\times 10^{-10}$ m in width in the presence of a high concentration of electrolye, only one monolayer of material adsorbed on the surface

could have any effect on E_H. However, from the capacitance data alone it is not possible to make an estimate of the absolute coverage on the electrodes; it is possible that an amount far less than a monolayer causes the shift in E_{FB}. We have examined this possibility with some simple calculations involving C_H, the Helmholtz capacity. The experimentally obtained voltage drop across the Helmholtz layer is related to C_H by eq 5, where Q_{ads} represents the total excess ionic change in the Helmholtz layer. Calculation of the Helmholtz capacity would allow an estimation of the quantity of the adsorbed charge; the formula for C_H/unit area is given in eq 11, where ϵ_0 is the primittivity of free space,

$$C_H = \epsilon_H \epsilon_0 / d \qquad (11)$$

d is the thickness of the Helmholtz layer, and ϵ_H is the dielectric constant of the Helmholtz layer. The double layer thickness is dependent on the concentration of electrolyte; at high concentrations, a value of (3–5) $\times 10^{-10}$ m is generally quoted. Factors that bear upon the dielectric constant of the Helmholtz layer of a semiconductor are not fully understood, but work using a value of C_H of approximately 1×10^{-5} F/cm^2 for an n-type semiconductor in CH_3CN has appeared.[20] Using this value and the observed shifts in E_{FB} from I of 1 V, one calculates a value for Q_{ads} of 10^{-5} C/cm^2. The charge density using an extreme upper limit for monolayer coverage of 10^{-9} mol/cm^2 is 9.6×10^{-5} C/cm^2, and thus the lower limit for the saturation coverage of I is 0.1 monolayer. When a more reasonable value for complete monolayer coverage of 10^{-10} mol/cm^2 is used, the experimental value for E_H indicates that all available adsorption sites are occupied at saturation; i.e., the coverage is one monolayer. For the other molecules, the saturation coverage is proportionately less according to the extent to which they shift E_{FB}, probably a consequence of the size of the molecules.

The conclusion that the saturation coverage of anion from I is about one monolayer accords well with the Auger spectroscopy illustrated in Figure 2. Coverages well below one monolayer are not easily observed with the Auger technique. The signal intensity for S for the adsorbed $Et_2NCS_2^-$ is consistent with substantial coverage of the surface.

(20) Kautek, W.; Gerischer, H. *Electrochim. Acta* **1982**, *27*, 1035.

Conclusions

Results reported in this article establish that it is possible to quantitatively measure adsorption of charged organic molecules onto semiconductors. The dithiocarbamates offer a rich source of molecules that can be investigated from the standpoint of geometric and electronic factors that may influence the strength of the binding and the coverage. Three dithiocarbamates have been used to show that both large changes in maximum coverage and binding energy can be achieved. For the three systems studied, size and solubility appear to be large factors in the variations observed. A simple Langmuir adsorption model appears to fit the experimental data for the cases studied. The fact that the neutral $[Et_2NC(S)S]_2$ does not adsorb to CdX (X = S, Se) and that less than 5 mM $Et_2NCS_2^-$ will give the maximum shift of E_{FB} accords well with the finding that the photoelectrochemical oxidation of $Et_2NCS_2^-$ occurs with high efficiency to large-extent conversion to $[Et_2NC(S)S]_2$. The strong interaction of CdX with the $Et_2NCS_2^-$ leads to a very large negative shift in E_{FB}, about 1 V, that allows the demonstration of very efficient conversion of optical energy to electrical energy to effect the desired oxidation process. Indeed, high efficiency for the conversion of light to electricity can be obtained for the n-CdX-based photoelectrochemical cells employing the $[Et_2NC(S)S]_2/[Et_2NH_2][Et_2NCS_2]$ redox couple, assuming that a reversible counterelectrode for the redox couple can be found. Part of the value of the redox couple is that it does not absorb in the visible region of the spectrum. Further, the negatively charged species interacts strongly with the photoanode to give large photovoltages, while the neutral oxidation product is innocent with respect to interaction with the CdS photoanodes.

Acknowledgment. We thank the United States Department of Energy, Office of Basic Energy Sciences, Division of Chemical Sciences for their support of this work. Use of the Central Facilities in the M.I.T. Center for Materials Science and Engineering supported by the NSF Materials Research Laboratory Program is also gratefully acknowledged.

Registry No. $Na[Et_2NCS_2]$, 148-18-5; $Na^+_2[CH_2N(Et)CS_2^-]_2$, 102261-38-1; $Na^+_2[CH_2CH_2CH_2N(Me)CS_2^-]$, 75854-55-6; $[Et_2NC(S)S]_2$, 97-77-8; CdS, 130-62-36; CdSe, 1306-24-7.